

A Closed-form Solution to Electromagnetic Sensor Based Intraoperative Limb Length Measurement in Total Hip Arthroplasty ^{*}

Tiancheng Li¹(✉), Yang Song¹, Peter Walker², Kai Pan¹, Victor A van de Graaf², Liang Zhao¹, and Shoudong Huang¹

¹ Robotics Institute, Faculty of Engineering and Information Technology, University of Technology Sydney, Ultimo, NSW 2007, Australia

`tiancheng.li-1@student.uts.edu.au`

² Concord Repatriation General Hospital, Concord, NSW 2139, Australia

Abstract. Total hip arthroplasty (THA) is an orthopaedic surgery to replace the diseased femoral head and socket of the hip joint with artificial implants. Achieving appropriate leg length and offset in THA is critical to avoid instability, leg length discrepancies, persistent pain, or early implant failure. This paper provides an electromagnetic (EM) sensor based approach for accurately measuring the change in leg length and offset intraoperatively. The proposed approach does not require direct line-of-sight, avoids the need for accurately returning the leg back to the neutral reference position, and has an efficient closed-form solution from least squares optimisation. Validations using simulations, phantom experiments, and cadaver tests demonstrate that the proposed method can provide more accurate results than the conventional method by manual gauge, the standard optical tracking based approach, and the direct use of one EM reading, thus showing significant potential clinical value.

1 Introduction

Hip osteoarthritis, with the top 10% occurrence in all diseases, brought a high demand for total hip arthroplasty (THA) in the past few decades [2]. According to the American Academy of Orthopaedic Surgeons, in the United States, approximately 450,000 THA surgeries are performed each year. One of the main challenges in THA is achieving accurate restoring leg length and femoral offset [3]. Failure in doing so can lead to instability, leg length discrepancies, impingement, persistent pain, and early implant failure [22], thus significantly affecting the clinical outcome and hip durability [19]. Therefore, a reliable intraoperative limb length measurement and restoration method is crucial to optimise patient outcomes and implant survival.

Intraoperatively, leg length and femoral offset can be determined manually using a calliper between two reference points [1, 3, 11, 17], but using a calliper is prone to measurement error [13]. Many computer-assisted methods [6] rely on

^{*} Supported by PMSW Research Pty Ltd, Australia.

numerous landmarks, such as condyles, or tibial spines, to determine the limb length [10], which could be inconvenient during surgeries. The optical tracking system is often used in THA for measurement as it has shown higher accuracy and reliability during interventions involving dynamic motion [18]. Sarin et al. [16] fixed optical tracking devices on the pelvis and femur as two references to measure the leg length and offset. Intellijoint HIP [13] is another 3D optical navigation tool, with the camera attached to the pelvis rather than placed next to the patient. Mako combines the preoperative CT 3D reconstruction and intraoperative optical tracking feedback for registration to determine the leg length and offset [4, 20]. The main limitation of optical tracking is the requirement for a direct and free line-of-sight between markers and cameras [18].

In contrast, the Electromagnetic (EM) sensor based navigation system can provide fast and accurate tracking without line-of-sight constraints [5, 18]. Zhao et al. [23] proposed a real-time robust simultaneous catheter and environment modelling for endovascular navigation, which is based on intravascular ultrasound and EM sensing. Mohammadbagherpoor et al. [12] developed an EM-based inductive proximity sensor system for detecting hip joint implant loosening in the micron range. Intracs^{®em} is an intelligent navigation system based on EM tracking for endoscopic minimally invasive spine surgery [8].

In the commonly used intraoperative leg length equalisation and offset recovery techniques, both traditional and computer-assisted methods require the femur to be held and stored at the preoperative neutral reference position (0° flexion, 0° rotation, and 0° abduction) prior to hip dislocation, and measure the changes in leg length and femoral offset as the femur is returned to the neutral reference position [1, 13, 15, 16]. Inaccurate repositioning of the femur w.r.t. the pelvis can result in additional measurement errors since only 4° of abduction/adduction could cause 5–7 *mm* error in leg length and 2–4 *mm* error in offset [9]. In our method, we aim to eliminate the femoral repositioning prior to measurement to avoid the additional errors.

In this work, we propose a robust and accurate intraoperative limb length measurement method for THA based on EM sensing. Using the idea that the femoral movement can be mathematically modelled as a vector rotating around a fixed rotation centre, we develop a closed-form optimisation solution that uses a set of sampled poses from EM readings to calculate the intraoperative limb length change. The experiment results demonstrate that the proposed method can be more accurate. In summary, the key advantages of our method include: (i) the optimisation with a closed-form solution is an active compensation [5, 18], which can effectively reduce static errors in the EM tracking itself and significantly improve the accuracy; (ii) different from pivot calibration, only slight movement of the femur is required to obtain accurate limb length measurements; (iii) no need to return the leg back to the neutral reference position again after replacing the damaged hip joint with artificial implants, which effectively avoids measurement errors due to inaccurate abduction/adduction repositioning; (iv) the proposed method does not require the direct line-of-sight, and can be easily integrated clinically, without interrupting the workflow of THA.

2 METHODOLOGY

2.1 Problem Formulation

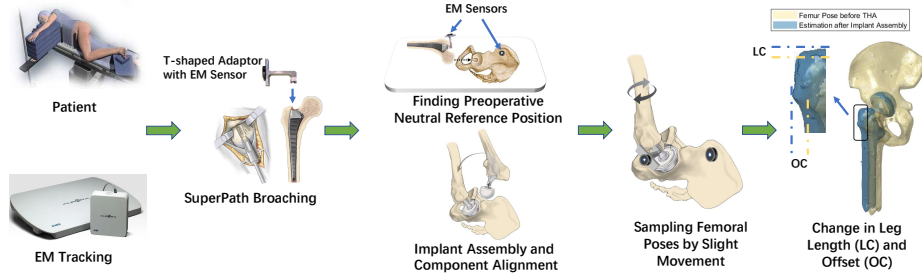


Fig. 1. The proposed EM-based intraoperative limb length measurement framework.

Standard THA Routine. During a standard THA, the surgery is often performed in the lateral position. Two reference points are marked on the pelvis and femur, respectively. The reference can be iliac fixation pins, sensors, or optical trackers. The surgeon then finds the preoperative neutral reference position by experience and records the relative position between the two reference points prior to the femoral head resection. The following routines include damaged femoral head removal, femoral canal broaching, acetabular preparation, and component selection and alignment. The component alignment requires the surgeon to return the femur to the neutral reference position and measure the change in leg length and offset.

Our Setup. In our proposed method (Fig. 1), the EM tracking board is placed under the patient’s hip during the THA surgery, and one pin with EM sensor is installed on the pelvis. The supercapsular percutaneously assisted (SuperPath) approach [14] is used to insert a metal stem (or implant) into the hollow centre of the femur, without the need for femoral head resection and removal prior to the femoral canal broaching. A T-shaped adaptor mounted with another EM sensor is rigidly attached to the stem. When measuring changes in leg length and femoral offset, we sample poses of the postoperative femur during a slight femoral movement. *The problem considered in this work is to use the sampling postoperative femoral poses to estimate the leg length and offset change instead of repositioning the femur to the neutral reference position.*

Denote the frames of EM sensors on the pelvis and femur as $\{P\}$ and $\{F\}$, respectively. The real-time readings of two EM sensors are represented as ${}^B\mathbf{X}_P = \{{}^B\mathbf{R}_P, {}^B\mathbf{t}_P\}$ and ${}^B\mathbf{X}_F = \{{}^B\mathbf{R}_F, {}^B\mathbf{t}_F\}$, which are respectively the rotation matrices and translation vectors of frames $\{P\}$ and $\{F\}$ w.r.t. the frame of EM tracking board denoted by $\{B\}$ (Fig. 2). Then, to eliminate the effect of patient motion, the relative pose of frame $\{F\}$ w.r.t. $\{P\}$ is used and denoted by ${}^P\mathbf{X}_F = \{{}^P\mathbf{R}_F, {}^P\mathbf{t}_F\}$, where ${}^P\mathbf{R}_F = {}^B\mathbf{R}_P^\top {}^B\mathbf{R}_F$ and ${}^P\mathbf{t}_F = {}^B\mathbf{R}_P^\top {}^B\mathbf{t}_F - {}^B\mathbf{t}_P$.

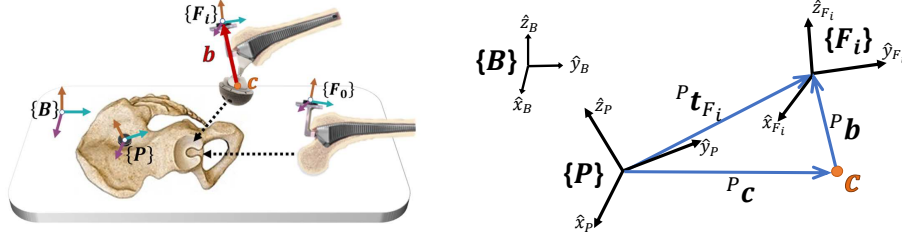


Fig. 2. Left: different coordinate frames involved in our THA setup; Right: relation among different vectors in (1).

Problem Statement. Suppose ${}^P\mathbf{X}_{F0}^{pre} = \{{}^P\mathbf{R}_{F0}^{pre}, {}^P\mathbf{t}_{F0}^{pre}\}$ is the recorded pose of $\{F\}$ w.r.t. $\{P\}$ at the preoperative neutral reference position before femoral head resection, and N sampling postoperative femoral poses in frame $\{P\}$, denoted by $\{{}^P\mathbf{X}_{Fi} = \{{}^P\mathbf{R}_{Fi}, {}^P\mathbf{t}_{Fi}\} \mid i \in \{1, \dots, N\}\}$, are collected through small motion around the neutral position after femoral head replacement. Since the relative rotations of frame $\{F\}$ in $\{P\}$ should be the same at the neutral reference position before and after the femoral head replacement, mathematically, the problem considered in this paper is, *given sampling postoperative femoral poses ${}^P\mathbf{X}_{Fi}$ ($i \in \{1, \dots, N\}$), accurately estimate the current translation vector ${}^P\mathbf{t}_{F0}^{post}$ when the relative rotation is ${}^P\mathbf{R}_{F0}^{pre}$, and then use it to calculate the change in leg length and offset.*

2.2 Limb Length Measurement without Femoral Repositioning

Since the joint between the acetabular component and the metal femoral head is a perfect sphere, the femoral movement in the frame $\{P\}$ can be mathematically modelled as a vector \mathbf{b} rotating around a centre \mathbf{c} (Fig. 2: Left), where \mathbf{c} is constant in frame $\{P\}$. Although \mathbf{b} is changing in $\{P\}$, it is a constant in $\{F\}$. Therefore, the relation among the vectors \mathbf{t} , \mathbf{b} , and \mathbf{c} (refer to Fig. 2: Right) can be described as

$${}^P\mathbf{t}_F = {}^P\mathbf{b} + {}^P\mathbf{c} = {}^P\mathbf{R}_F {}^F\mathbf{b} + {}^P\mathbf{c}, \quad (1)$$

where ${}^P\mathbf{b}$ and ${}^F\mathbf{b}$ are the rotating vector \mathbf{b} in $\{P\}$ and $\{F\}$, respectively, and ${}^P\mathbf{c}$ is the rotation centre \mathbf{c} in $\{P\}$.

The relation (1) is valid for all ${}^P\mathbf{X}_F$, so ${}^F\mathbf{b}$ and ${}^P\mathbf{c}$ can be obtained from the N sampled poses ${}^P\mathbf{X}_{Fi}$ ($i \in \{1, \dots, N\}$) by solving an optimisation problem. Then, the postoperative translation vector ${}^P\mathbf{t}_{F0}^{post}$ can be calculated by the relative rotation ${}^P\mathbf{R}_{F0}^{pre}$. In contrast to pivot calibration [21] which is commonly used to estimate the tip location of a pointer tool, our method focuses on estimating limb change after femoral head replacement and therefore requires only minor leg movements for sampling, and inaccurate rotation centre estimate due to singularity has almost no effect on limb length estimation. See below for details.

Full Least Squares Solution. Through the iterative Gauss-Newton (GN) method, the solution for ${}^F\mathbf{b}$ and ${}^P\mathbf{c}$ can be obtained by solving the following

full nonlinear least squares (Full LS) optimisation problem,

$$\arg \min_{{}^F \mathbf{b}, {}^P \mathbf{c}, {}^P \bar{\mathbf{R}}_{F_i}} \sum_{i=1}^N \left\| {}^P \bar{\mathbf{R}}_{F_i} {}^F \mathbf{b} + {}^P \mathbf{c} - {}^P \mathbf{t}_{F_i} \right\|_{\boldsymbol{\Omega}_{ti}^{-1}}^2 + \left\| r({}^P \bar{\mathbf{R}}_{F_i}) - r({}^P \mathbf{R}_{F_i}) \right\|_{\boldsymbol{\Omega}_{Ri}^{-1}}^2, \quad (2)$$

where $r({}^P \mathbf{R}_{F_i})$ and $r({}^P \bar{\mathbf{R}}_{F_i})$ are the Euler angles of rotation measurement ${}^P \mathbf{R}_{F_i}$ and the corresponding rotation variable ${}^P \bar{\mathbf{R}}_{F_i}$, respectively. $\boldsymbol{\Omega}_{ti}$ and $\boldsymbol{\Omega}_{Ri}$ are the covariance matrices of EM measurement noises w.r.t. translation and rotation.

Closed-form Solution. Since the EM measurements of rotations are accurate enough [7], i.e. ${}^P \bar{\mathbf{R}}_{F_i} \approx {}^P \mathbf{R}_{F_i}$, the contribution of the second term in (2) is limited. As a result, the optimisation problem can be simplified as a linear least squares problem by letting ${}^P \bar{\mathbf{R}}_{F_i} = {}^P \mathbf{R}_{F_i}$:

$$\arg \min_{{}^F \mathbf{b}, {}^P \mathbf{c}} \sum_{i=1}^N \left\| {}^P \mathbf{R}_{F_i} {}^F \mathbf{b} + {}^P \mathbf{c} - {}^P \mathbf{t}_{F_i} \right\|_{\boldsymbol{\Omega}_{ti}^{-1}}^2, \quad (3)$$

which has an easier and more efficient closed-form solution

$$\begin{bmatrix} {}^F \mathbf{b}^* \\ {}^P \mathbf{c}^* \end{bmatrix} = \begin{bmatrix} \sum_{i=1}^N {}^P \mathbf{R}_{F_i}^\top \boldsymbol{\Omega}_{ti}^{-1} {}^P \mathbf{R}_{F_i} & \sum_{i=1}^N {}^P \mathbf{R}_{F_i}^\top \boldsymbol{\Omega}_{ti}^{-1} \\ \sum_{i=1}^N \boldsymbol{\Omega}_{ti}^{-1} {}^P \mathbf{R}_{F_i} & \sum_{i=1}^N \boldsymbol{\Omega}_{ti}^{-1} \end{bmatrix}^{-1} \begin{bmatrix} \sum_{i=1}^N {}^P \mathbf{R}_{F_i}^\top \boldsymbol{\Omega}_{ti}^{-1} {}^P \mathbf{t}_{F_i} \\ \sum_{i=1}^N \boldsymbol{\Omega}_{ti}^{-1} {}^P \mathbf{t}_{F_i} \end{bmatrix}. \quad (4)$$

The comparison in Section 3 will show that the closed-form solution (4) is almost the same as the solution to Full LS (2), but only requires sub-millisecond computational cost which is thousands of times less. Closed-form solution also benefits from the fact that solutions can be obtained in one step, avoiding potential local minima, providing greater robustness, and being easier to implement. So our proposed measurement approach is based on the closed-form solution.

Limb Length Change Measurement. After ${}^F \mathbf{b}^*$ and ${}^P \mathbf{c}^*$ are obtained, the postoperative translation vector ${}^P \mathbf{t}_{F_0}^{post}$ at neutral reference position (where the relative rotation is ${}^P \mathbf{R}_{F_0}^{pre}$) can be calculated by (1)

$${}^P \mathbf{t}_{F_0}^{post} = {}^P \mathbf{R}_{F_0}^{pre} {}^F \mathbf{b}^* + {}^P \mathbf{c}^*. \quad (5)$$

The change of relative translation vector at the neutral reference position is $\Delta {}^P \mathbf{t}_{F_0} = {}^P \mathbf{t}_{F_0}^{post} - {}^P \mathbf{t}_{F_0}^{pre}$. Further, we denote ${}^P \mathbf{L}$ as the projection of $\Delta {}^P \mathbf{t}_{F_0}$ onto the sagittal plane. Then, the changes in leg length and offset are computed by the norms $\|{}^P \mathbf{L}\|$ and $\|\Delta {}^P \mathbf{t}_{F_0} - {}^P \mathbf{L}\|$, respectively.

The covariance of ${}^P \mathbf{t}_{F_0}^{post}$ in (5) is calculated by

$$\boldsymbol{\Omega}_{P \mathbf{t}_{F_0}^{post}} = \left[{}^P \mathbf{R}_{F_0}^{pre \top} \mathbf{I} \right] \left(\sum_{i=1}^N \left[{}^P \mathbf{R}_{F_i}^\top \mathbf{I} \right]^\top \boldsymbol{\Omega}_{ti}^{-1} \left[{}^P \mathbf{R}_{F_i}^\top \mathbf{I} \right] \right)^{-1} \left[{}^P \mathbf{R}_{F_0}^{pre \top} \mathbf{I} \right]^\top, \quad (6)$$

where \mathbf{I} is the identity matrix, $\boldsymbol{\Omega}_{ti}$ is the covariance matrices of EM measurement noises w.r.t. translation. It can be proved that (6) tends to be zero as increasing samples if data are all sampled around the neutral position (${}^P \mathbf{R}_{F_i} \approx {}^P \mathbf{R}_{F_0}^{pre}$), although the uncertainty of ${}^F \mathbf{b}^*$ and ${}^P \mathbf{c}^*$ in (4) is large due to the near singularity in this case. Therefore, a slight movement of the leg (rotating around the neutral position within a few degrees) can guarantee the accuracy of limb length estimate while preventing injury to the patient and the workload of surgeons.

3 EXPERIMENTS

3.1 Simulation and Robustness Assessment

To compare the closed-form solution (4) and the solution to Full LS (2), five different levels of zero-mean Gaussian noises are added to the rotation angles and translations of sampling femoral poses ${}^P\mathbf{X}_{F_i}$ ($i \in \{1, \dots, 100\}$) from EM readings (first row in Tab. 1). Twenty independent runs are executed for each noise level to test the robustness and accuracy of both two methods. The mean absolute errors compared with the ground truth and standard deviation (STD) of the twenty runs for estimating the neutral femur position are shown in Tab. 1. It shows that the proposed closed-form solution can achieve similar accuracy compared with the solution to the Full LS problem and the robustness to additionally added sensor noises is high.

Table 1. Estimation error and STD from simulations with five increasing noise levels.

Noises: {Rot, Trans}	{0.1 rad, 2 mm}	{0.2 rad, 4 mm}	{0.3 rad, 6 mm}	{0.4 rad, 8 mm}	{0.5 rad, 10 mm}
Closed-form (mm)	0.2276 (0.0885)	0.7896 (0.3405)	1.4935 (0.8403)	1.9496 (0.7359)	2.7028 (1.1972)
Full LS (mm)	0.2272 (0.0887)	0.7878 (0.3408)	1.4886 (0.8397)	1.9412 (0.7361)	2.6910 (1.1971)

3.2 Phantom Experiments

The phantom experiments (Fig. 3) were performed using two different sawbones models. One experienced surgeon executed a normal surgical routine using standard hip arthroplasty components. Three commonly used standard femoral heads ($\{-4, 0, +4\}$ mm) were used for the alignment (Fig. 3: Right). After placing a metal acetabular shell into the pelvic cavity and inserting a stem into the femur, the surgeon selected one femoral head component and placed it on top of the stem, and the femoral head was placed into the liner. Then the surgeon found

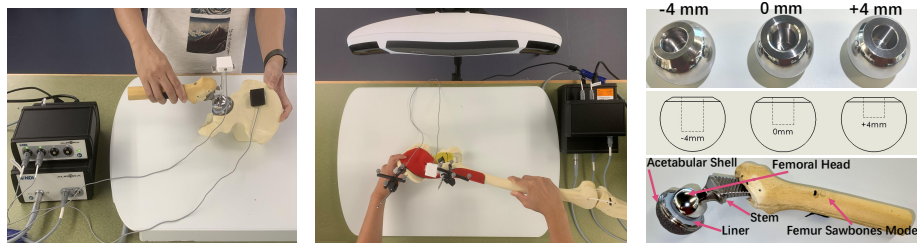


Fig. 3. Left: the first setup for comparison between closed-form solution (4) and solution to Full LS (2); Middle: the second setup for comparison of the proposed method to the other three methods (manual gauge, optical tracking, and one EM reading); Right: standard hip arthroplasty components used in phantom experiments.

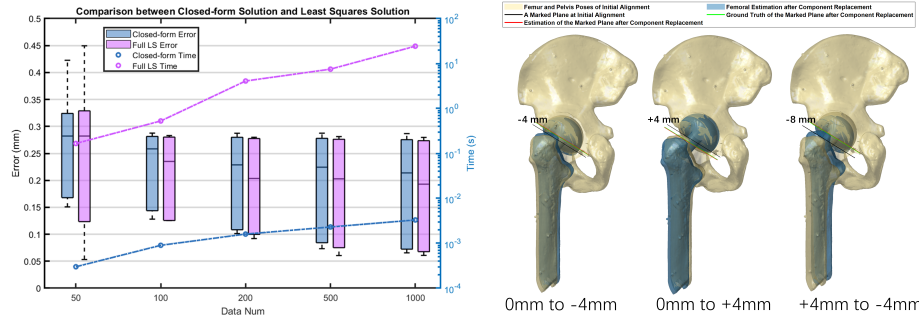


Fig. 4. Results from the first phantom experiment setup (Fig. 3: Left). Left: comparison between closed-form solution (4) and solution to Full LS (2); Right: femur pose estimation with closed-form solution (using 100 data) for three different alignments.

Table 2. Comparison of the proposed method to the other three methods in the second phantom experiment setup (Fig. 3: Middle).

Setups	-4 to 0		-4 to +4		0 to -4		0 to +4		+4 to -4		+4 to 0		p -value
MAE (mm)	LC	OC	LC	OC	LC	OC	LC	OC	LC	OC	LC	OC	
Closed-form	0.25	0.35	0.21	0.40	0.28	0.22	0.14	0.13	0.17	0.21	0.02	0.15	-
Optical Tracking	1.14	1.99	2.58	2.38	3.04	0.54	1.30	0.41	0.99	0.66	0.39	0.73	3.35e-4
One EM Reading	3.18	1.19	4.45	1.94	2.76	0.75	1.50	0.71	1.87	1.47	0.70	0.80	1.27e-4
Manual Gauge	3.19	2.35	6.23	4.58	3.86	0.82	1.73	1.36	2.30	1.81	1.47	1.86	2.38e-5

and recorded the neutral reference position of the femur model. After that, another femoral head was replaced to change the limb length. Finally, the limb length change before and after the femoral component replacement was calculated by different methods. The ground truth was available from the size changes between femoral head components.

Number of Samples and Comparison with Full LS. The first setup of phantom experiments (Fig. 3: Left) was designed to analyse the effect of the number of sampled poses on the performance of our method and to further compare the closed-form solution (4) and the solution to Full LS (2). Six different alignments of the femoral head components were performed (-4 to 0, -4 to +4, 0 to -4, 0 to +4, +4 to -4, and +4 to 0). After installing the replaced femoral head components, the surgeon slightly rotated the femur to collect the sampling pose data from EM sensors ($\{50, 100, 200, 500, 1000\}$ samples for each alignment). As shown in Fig. 4: Left, the closed-form solution performs as good as Full LS, with computational costs ranging from 0.3 ms to 3.3 ms corresponding to data numbers of 50 to 1000, which is thousands of times less than Full LS. Estimation error decreases as the number of samples increases. Three examples of results are shown in Fig. 4: Right. The acquisition frequency of EM tracking is 20 Hz and the improvement in accuracy is limited when the number of data is more than 100. To balance the efficiency and accuracy, the closed-form solution with 100 data is our choice for the experiments in the rest of the paper.

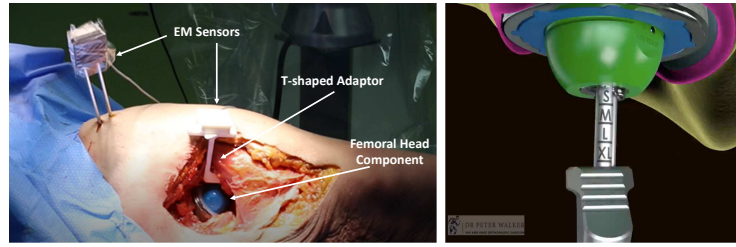


Fig. 5. Left: cadaver experiment; Right: an adjustable trial neck that can align limb length without the need to dislocate the hip to change the head.

Comparison with Other Methods. We compared our proposed method (Closed-form) with three other different measurement approaches in the second phantom experiment setup (Fig. 3: Middle). The standard optical tracking based approach [13, 16], the conventional mechanical method [1, 3, 11, 17] by manual gauge, and our method, were performed at the same time. A straightforward idea of using EM sensor (one EM reading only) was also carried out to demonstrate the advantage of our closed-form solution further. The groin pins, optical trackers, and EM sensors were fixed on the sawbones models. All three methods other than ours require repositioning the femur to the neutral reference position before measurements. Tab. 2 summarises the mean absolute errors (MAE) of leg length change (LC) and offset change (OC) using all methods for six different alignments. Three independent runs are executed for each alignment and overall the proposed method achieves the highest accuracy (the p -values for the other three methods compared to ours are shown in the last column of Tab. 2).

3.3 Cadaver Experiments

The proposed method was also tested in cadaver experiments (Fig. 5: Left). The cadaveric body was operated on lateral decubitus. The whole THA routines including SuperPath broaching, hip dislocation, femoral head removal as well as acetabular and femoral preparation were executed in the cadaver experiment. To conduct multiple sets of experiments, a standard adjustable trial neck (Fig. 5: Right) was inserted which allowed limb length changes without dislocating and altering the femoral head. Finally, the cadaver experiment yielded eight sets of alignments by changing the trial neck length. As shown in Tab. 3, the proposed method can reach a mean absolute error (MAE) of about 0.4 mm, which is much smaller than directly using one EM reading.

Table 3. Cadaver Experiment

Datasets	1		2		3		4		5		6		7		8		MAE (STD)			
Errors (mm)	LC	OC	LC	OC	LC	OC	LC	OC	LC	OC	LC	OC	LC	OC	LC	OC	LC	OC		
Closed-form	0.51	0.41	0.42	0.34	0.36	0.28	0.01	0.02	0.35	0.28	0.70	0.56	0.38	0.30	0.60	0.48	0.42	(0.21)	0.33	(0.16)
One EM Reading	1.13	0.98	0.52	1.40	0.74	1.32	1.45	1.55	2.64	1.47	2.99	1.59	4.21	3.73	3.21	2.35	2.11	(1.34)	1.80	(0.87)

4 Conclusion

This paper presents an efficient closed-form solution based on EM sensing to robustly and accurately calculate the intraoperative change in leg length and offset. Simulations, phantom experiments, and cadaver tests demonstrate the efficiency and accuracy of our proposed algorithm compared to the conventional manual gauge method and standard optical tracking based method, showing the potential value in clinical practice. The reasons why the proposed solution can significantly improve the accuracy are: (i) it uses a set of sampled poses from EM readings to optimise the intraoperative limb length change instead of only using one sensor reading; (ii) there is no requirement of repositioning the femur to the neutral position before the measurements. The computational time of our method is only around 0.3 ms mainly due to the closed-form solution.

Some studies assessed that metals in the surgical environment might affect the accuracy of EM tracking [18]. However, the design of EM is not affected by titanium and 300 series stainless steel, which are the main materials of surgical instruments used in THA, and our cadaver experiments in a surgical environment have shown that our method still guarantees measurement accuracy (the mean absolute error is around 0.4 mm). In the future, we aim to further validate our approach through clinical trials and have plans to extend the EM-based intraoperative limb length measurement to total knee arthroplasty surgery.

References

1. Bose, W.J.: Accurate limb-length equalization during total hip arthroplasty. *Orthopedics* **23**(5), 433 (2000)
2. Cross, M., Smith, E., Hoy, D., Nolte, S., Ackerman, I., Fransen, M., Bridgett, L., Williams, S., Guillemin, F., Hill, C.L., et al.: The global burden of hip and knee osteoarthritis: estimates from the global burden of disease 2010 study. *Annals of the rheumatic diseases* **73**(7), 1323–1330 (2014)
3. Desai, A.S., Dramis, A., Board, T.N.: Leg length discrepancy after total hip arthroplasty: a review of literature. *Current reviews in musculoskeletal medicine* **6**, 336–341 (2013)
4. Fontalis, A., Kayani, B., Thompson, J.W., Plastow, R., Haddad, F.S.: Robotic total hip arthroplasty: Past, present and future. *Orthopaedics and Trauma* **36**(1), 6–13 (2022)
5. Franz, A.M., Haidegger, T., Birkfellner, W., Cleary, K., Peters, T.M., Maier-Hein, L.: Electromagnetic tracking in medicine—a review of technology, validation, and applications. *IEEE transactions on medical imaging* **33**(8), 1702–1725 (2014)
6. Gheewala, R.A., Young, J.R., Villacres Mori, B., Lakra, A., DiCaprio, M.R.: Perioperative management of leg-length discrepancy in total hip arthroplasty: a review. *Archives of Orthopaedic and Trauma Surgery* pp. 1–7 (2023)
7. Gomes-Fonseca, J., Veloso, F., Queirós, S., Morais, P., Pinho, A.C., Fonseca, J.C., Correia-Pinto, J., Lima, E., Vilaça, J.L.: Assessment of electromagnetic tracking systems in a surgical environment using ultrasonography and ureteroscopy instruments for percutaneous renal access. *Medical Physics* **47**(1), 19–26 (2020)

8. Hagan, M.J., Remacle, T., Leary, O.P., Feler, J., Shaaya, E., Ali, R., Zheng, B., Bajaj, A., Traupe, E., Kraus, M., et al.: Navigation techniques in endoscopic spine surgery. *BioMed Research International* **2022** (2022)
9. Kawamura, H., Watanabe, Y., Nishino, T., Mishima, H.: Effects of lower limb and pelvic pin positions on leg length and offset measurement errors in experimental total hip arthroplasty. *Journal of Orthopaedic Surgery and Research* **16**(1), 1–9 (2021)
10. Lecoanet, P., Vargas, M., Pallaro, J., Thelen, T., Ribes, C., Fabre, T.: Leg length discrepancy after total hip arthroplasty: can leg length be satisfactorily controlled via anterior approach without a traction table? evaluation in 56 patients with eos 3d. *Orthopaedics & Traumatology: Surgery & Research* **104**(8), 1143–1148 (2018)
11. McGee, H., Scott, J.: A simple method of obtaining equal leg length in total hip arthroplasty. *Clinical orthopaedics and related research* (194), 269–270 (1985)
12. Mohammadbagherpoor, H., Ierymenko, P., Craver, M.H., Carlson, J., Dausch, D., Grant, E., Lucey, J.D.: An implantable wireless inductive sensor system designed to monitor prosthesis motion in total joint replacement surgery. *IEEE Transactions on Biomedical Engineering* **67**(6), 1718–1726 (2019)
13. Paprosky, W.G., Muir, J.M.: Intellijoint hip®: a 3d mini-optical navigation tool for improving intraoperative accuracy during total hip arthroplasty. *Medical Devices: Evidence and Research* pp. 401–408 (2016)
14. Quitmann, H.: Supercapsular percutaneously assisted (superpath) approach in total hip arthroplasty. *Operative Orthopädie und Traumatologie* **31**(6), 536–546 (2019)
15. Renkawitz, T., Schuster, T., Grifka, J., Kalteis, T., Sendtner, E.: Leg length and offset measures with a pinless femoral reference array during tha. *Clinical Orthopaedics and Related Research®* **468**(7), 1862–1868 (2010)
16. Sarin, V.K., Pratt, W.R., Bradley, G.W.: Accurate femur repositioning is critical during intraoperative total hip arthroplasty length and offset assessment. *The Journal of arthroplasty* **20**(7), 887–891 (2005)
17. Shiramizu, K., Naito, M., Shitama, T., Nakamura, Y., Shitama, H.: L-shaped caliper for limb length measurement during total hip arthroplasty. *The Journal of bone and joint surgery. British volume* **86**(7), 966–969 (2004)
18. Sorriento, A., Porfido, M.B., Mazzoleni, S., Calvosa, G., Tenucci, M., Ciuti, G., Dario, P.: Optical and electromagnetic tracking systems for biomedical applications: A critical review on potentialities and limitations. *IEEE reviews in biomedical engineering* **13**, 212–232 (2019)
19. Takamatsu, T., Shishido, T., Takahashi, Y., Masaoka, T., Tateiwa, T., Kubo, K., Endo, K., Aoki, M., Yamamoto, K.: Radiographic determination of hip rotation center and femoral offset in japanese adults: a preliminary investigation toward the preoperative implications in total hip arthroplasty. *BioMed Research International* **2015** (2015)
20. Tarwala, R., Dorr, L.D.: Robotic assisted total hip arthroplasty using the mako platform. *Current reviews in musculoskeletal medicine* **4**, 151–156 (2011)
21. Yaniv, Z.: Which pivot calibration? In: *Medical imaging 2015: Image-guided procedures, robotic interventions, and modeling*. vol. 9415, pp. 542–550. SPIE (2015)
22. Zahar, A., Rastogi, A., Kendoff, D.: Dislocation after total hip arthroplasty. *Current reviews in musculoskeletal medicine* **6**, 350–356 (2013)
23. Zhao, L., Giannarou, S., Lee, S.L., Yang, G.Z.: Scem+: real-time robust simultaneous catheter and environment modeling for endovascular navigation. *IEEE Robotics and Automation Letters* **1**(2), 961–968 (2016)